Article

Rh(III)-Catalyzed and Solvent-Controlled Chemoselective Synthesis of Chalcone and Benzofuran Frameworks via Synergistic Dual Directing Groups Enabled Regioselective C–H Functionalization: a Combined Experimental and Computational Study

Wei Yi, Weijie Chen, Fu-Xiaomin Liu, Yuting Zhong, Dan Wu, zhi Zhou, and Hui Gao

ACS Catal., **Just Accepted Manuscript** • DOI: 10.1021/acscatal.8b02402 • Publication Date (Web): 05 Sep 2018

Rh(III)-Catalyzed and Solvent-Controlled Chemoselective Synthesis of Chalcone and Benzofuran Frameworks via Synergistic Dual Directing Groups Enabled Regioselective C–H Functionalization: a Combined Experimental and Computational Study

Wei Yi,[†,*] Weijie Chen,[†] Fu-Xiaomin Liu,[†] Yuting Zhong,[†] Dan Wu,[†] Zhi Zhou,[†,*] and Hui Gao[†,‡,*]

Dedicated to Professor Xiyan Lu on the occasion of his 90th birthday

[†]Key Laboratory of Molecular Target & Clinical Pharmacology, School of Pharmaceutical Sciences & the Fifth Affiliated Hospital, Guangzhou Medical University, Guangzhou, Guangdong 511436, China
[‡] School of Pharmaceutical Sciences, Sun Yat-sen University, Guangzhou, 510006, China
Supporting Information Placeholder

ABSTRACT: By virtue of a synergistically dual directing groups (the O–NHAc part and the hydroxyl group)-assisted strategy, the efficient and practical Rh(III)-catalyzed regioselective redox-neutral C–H functionalization of diverse *N*-phenoxyacetamides with propargyl alcohols has been realized, which led to the divergent synthesis of privileged benzofuran and chalcone frameworks in a solvent-controlled chemoselective manner. Experimental and computational studies reveal that the formation of the hydrogen bonding between dual directing groups and the subsequent coordination interaction between the hydroxyl group and the Rh(III) catalyst play a decisive role in promoting the regioselective migratory insertion of the alkyne moiety. Thereafter, two solvent-controlled switchable reaction pathways which respectively involve tandem *β*–H elimination/hydrogen transfer/oxidative addition/C–O bond reductive elimination/oxidation (for low-polar solvents: path **I**-**I$_a$** via a Rh^{III}-Rh^{I}-Rh^{III} pathway) and oxidative addition/β–H elimination/hydrogen transfer/protonolysis (for high-polar solvents: path **II**-**II$_b$** via a Rh^{III}-Rh^{V}-Rh^{III} pathway), are followed to deliver the corresponding products with excellent chemoselectivity. Taken together, our results presented here not only give a remarkable and meaningful expansion in the area of O–NHAc-directed C–H activations but also provide a rational basis for future development of synergistic dual DGs-enabled C–H functionalization reactions.
KEYWORDS: *Rh(III) catalyst, N-phenoxyacetamides, propargyl alcohols, benzofurans, chalcones, experimental and computational studies*

INTRODUCTION

The directing group (DG)-assisted and transition metal (TM)-catalyzed C–H functionalization has become a powerful, straightforward and regioselective approach that relies on simple and readily available starting inputs for the construction of a variety of organic building blocks via the cleavage of inert C–H bond and the final formation of new C–C or C–X bonds.[1] In direct C–H bond functionalization, the chelation-assisted *ortho*-metalation is typically involved to yield a nucleophilic metallacycle complex as the active intermediate, which adds across with a valuable coupling partner (CP) to generate an ideal and functionalized product. Up to date, a large number of versatile DGs as well as CPs have been developed for the diverse C–H bond transformations.[2-3] Despite the remarkable advances in this field, further exploration of novel chelation-assisted strategy for achieving the effective and characteristic C–H functionalization is still highly desirable, especially for the direct construction of privileged structural motifs. In this regard, recently developed bidentate chelating auxiliaries[4-7] have emerged as one of the most attractive strategies to realize some elegant and important transformations with the controllable regioselectivity, in which the conventional monodentate DG remains unsolved. Indeed, such strategy can confer to the new property of the metallacycle complex, thus leading to the discovery of novel and regioselective C–H activation mode (Scheme 1a). Unfortunately, the bidentate chelating auxiliaries reported in TM-catalyzed C–H functionalization are limited to N,N-,[4d,5] N,O-[6] or N,S-based[7] skeletons and often need strict spatial dimension for achieving the coordination with the TM, which lead inevitably to relatively poor product diversity in comparison with monodentate DGs.

To address these drawbacks, very recently a synergetic dual DGs-directed strategy containing both a conventional monodentate DG and a traceless DG attached in the CPs has been developed by Glorius group[8] to furnish the

expected bidentate coordination (Scheme 1b). In principle, the conventional monodentate DG enables chelation-assisted C–H activation, and the introduction of the second traceless DG at the CP moiety plays a crucial role in controlling the regioselectivity and/or improving the reactivity. However, to the best of our knowledge, very few TM-catalyzed examples[8,9] that only used Mn(I) or Ir(III) as the catalyst have been reported so far. To a certain extent, it might be due to the lack of a clear and basic mechanism for understanding such synergetic strategy-based C–H activation mode and action.

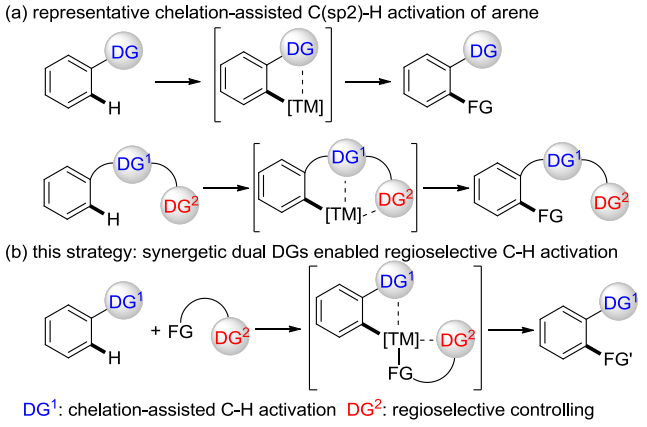

Scheme 1. Chelation-Assisted TM-Catalyzed C-H Activation

In a search for appropriate CPs equipped with chelating auxiliaries, we turned our attention to propargyl alcohols, which are easily accessible and have been precedently proven to be good reactants for TM-catalyzed C–H functionalization.[10] Moreover, because of the binding affinity potential of the hydroxyl group with the TM catalyst, they can be viewed as promising chelating CPs. In our previous work, we have revealed the switchable [3+2] and [4+2] annulations of oximes with using tertiary propargyl alcohols as the CPs, in which the hydroxyl group provided distinctive interactions with different TM catalysts to affect the regio- and chemoselectivity of the reaction.[9a] Further expansion of the versatile CPs to the *N*-phenoxyacetamide substrates has also been achieved under the Ir(III) catalysis.[9b]

On the basis of the above information and in continuation of our interest in Rh(III)-catalyzed C–H functionalization, herein, we aim to report the first Rh(III)-catalyzed, solvent-controlled, redox-neutral, regioselective C–H functionalization of *N*-phenoxyacetamides with new type of chelating propargyl alcohols (readily available primary or secondary propargyl alcohols) using a synergetic dual DGs-enabled regioselective strategy for the divergent and chemoselective synthesis of benzofurans and chalcones, two privileged core structural motifs widely found in natural products, organic materials and biologically active compounds.[11] Through a series of experimental investigations together with detailed theoretical studies, the role of the hydroxyl group in propargyl alcohols and the origin of the chemoselectivity were clarified. Besides, the distinctive catalytic modes for the divergent synthesis of the related products by following two novel and different reaction pathways (respectively named path **I-I$_a$** (via a Rh^{III}-Rh^{I}-Rh^{III} pathway) and path **II-II$_b$** (via a Rh^{III}-Rh^{V}-Rh^{III} pathway) were also deduced rationally.

RESULTS AND DISCUSSION

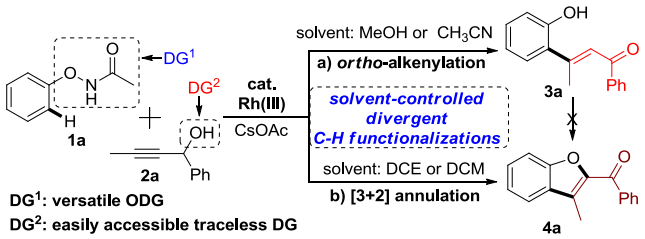

Scheme 2. Rh(III)-Catalyzed Divergent C–H Functionalization of *N*-Phenoxyacetamides with Tunable Selectivity

Solvent-Controlled Divergent C–H functionalization of *N*-Phenoxyacetamides with Propargyl Alcohols. *Method Development.* The O–NHAc part represents one of the versatile oxidizing directing groups (ODGs) for the redox-neutral coupling with various reagents including alkynes,[12] alkenes,[13] diazo compounds,[14] and other CPs.[15] Precedent literatures have well-addressed the divergent C–H functionalization of *N*-phenoxyacetamides with proper CPs via selective C–N or C–O bond reductive elimination.[12-15] Based on these and inspired by the emerging synergistically dual DGs-directed strategy, we herein employ readily available propargyl alcohols as the chelating partners to react with *N*-phenoxyacetamides bearing a monodentate –ONHAc ODG, expecting to develop the novel reaction mode and obtain the interesting product structure. At the outset of our investigation, *N*-phenoxyacetamide (**1a**) and 1-phenylbut-2-yn-1-ol (**2a**) were chosen as the model substrates and the reaction was carried out under the Rh(III) catalysis (see Tables S1 and S2 in the Supporting Information for details). To our delight, with methanol being the solvent, the reaction proceeded smoothly under the initial conditions to deliver a free hydroxyl-substituted chalcone **3a** in the presence of [Cp*RhCl$_2$]$_2$ and CsOAc. Very interestingly, further screening of various experimental parameters indicated that the solvent exerted a crucial influence on the reaction outcome. With the high-polar solvents being the reaction medium such as methanol and CH$_3$CN, the chalcone derivative **3a** was obtained as the main product via the *ortho*-alkenylation, while an alternative [3+2] annulation process was achieved by simply switching the solvents to low-polar DCE or DCM, leading to the efficient synthesis of benzofuran derivative **4a** (Scheme 2). Noteworthily, further examination indicated that **3a** could not be converted to **4a** under the reaction conditions, revealing that two different mechanisms

might be involved in the solvent-controlled divergent C–H functionalization reactions.

Table 1. Examinations of the Solvent Effect[a]

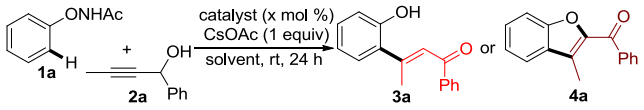

Entry	Catalyst (x mol %)	Solvent	Yield[b] (%) 3a	4a
1	[Cp*RhCl2]2 (5)	MeOH	36	/
2	[Cp*RhCl2]2 (5)	EtOH	41	/
3	[Cp*RhCl2]2 (5)	iPrOH	30	<5
4	[Cp*RhCl2]2 (5)	dioxane	51	<5
5	[Cp*RhCl2]2 (5)	DMA	27	/
6	[Cp*RhCl2]2 (5)	THF	53	<5
7	[Cp*RhCl2]2 (5)	acetone	55	<5
8	[Cp*RhCl2]2 (5)	CH3CN	57	<5
9	[Cp*RhCl2]2 (5)	toluene	26	36
10	[Cp*RhCl2]2 (5)	DCE	24	47
11	[Cp*RhCl2]2 (5)	DCM	10	53
12[c]	[Cp*RhCl2]2 (5)	CH3CN	81	/
13[d,e]	[Cp*RhCl2]2 (5)	DCM	/	84
14	[Cp*IrCl2]2 (5)	CH3CN/DCM	NR	
15	Cp*Co(CO)I2 (10)	CH3CN/DCM	NR	
16	[CyRuCl2]2 (5)	CH3CN/DCM	NR	
17	Mn(CO)5Br (10)	CH3CN/DCM	NR	

[a]Reaction conditions: **1a** (0.2 mmol), **2a** (0.2 mmol), $[Cp^*RhCl_2]_2$ (5 mol %) and CsOAc (1 equiv) in solvent (0.1 M) at room temperature for 24 h under air. [b]Isolated yield. [c]2 equiv of 2a was used. [d]1.5 equiv of 2a was used, the reaction was conducted at 50 °C. [e]NaOAc (1 equiv) was used instead of CsOAc.

Enlightened by the tunable selectivity and the synthetic utility potential for the efficient construction of chalcones and benzofurans, we next screened the experimental parameters systemically to figure out the optimal reaction conditions as well as the effect of the solvent.[16] As shown in Table 1, a series of organic solvents including alcohols, ethers and halohydrocarbons were tested, showing that chalcone derivative **3a** was obtained as the dominant product in most of the high-polar solvents, among which CH_3CN resulted in the highest yield up to 57% (entry 8). However, when the low-polar solvents such as toluene, DCE and DCM was respectively subjected to the reaction conditions with the same substrates, a mixture of **3a** and cyclized benzofuran product **4a** was obtained, among which DCM gave the best chemoselectivity, affording **4a** in 53% yield (entry 11). Further screening of additives, reaction temperature as well as the proportion of substrates resulted in the optimal conditions for both products, thus providing an efficient solvent-controlled strategy for the divergent synthesis of chalcone and benzofuran derivatives (entries 12 and 13). As a comparison, other TM catalysts which showed good reaction activities and diversities in precedent literatures[17] including Ir(III), Ru(II), Co(III) and Mn(I) species were also screened and seemed to be totally ineffective (entries 14-17), reflecting the high efficiency and indispensability of $[Cp^*RhCl_2]_2$ for these transformations.

Scope of the C–H Alkenylation Reaction for the Synthesis of Chalcone Derivatives. With the optimal reaction conditions established, we started to investigate the scope and generality of this methodology for the efficient synthesis of chalcones by screening a series of substrates bearing kinds of functional groups with different steric and electrical properties. Firstly, a variety of substituted *N*-phenoxyacetamides were assessed for this transformation by using CH_3CN as the solvent (Scheme 3). Gratifyingly, the developed Rh(III)-catalyzed system proved to be broadly applicable, and various commonly encountered functional groups including alkyl- (**3b-c**, **3j**, **3l-m**), halogens- (**3d-g**, **3k**), cyano- (**3h**) and ester-substituted *N*-phenoxyacetamides (**3i**) were well tolerated to deliver the corresponding products in moderate to good yields. Summarizing all these substrates, a significant electronic effect could be deduced qualitatively since *N*-phenoxyacetamides bearing the electron-withdrawing group gave relatively low yields compared with those bearing the electron-donating group. Of note, when *meta*-substituted *N*-phenoxyacetamides were employed, the reaction proceeded smoothly and provided the desired products in good yields with exclusive regioselectivities toward the less-hindered site (**3j-l**), while *ortho*-methyl-substituted *N*-phenoxyacetamide **1m** led to a low yield of the corresponding chalcone derivative, demonstrating that the position of substituent on the phenyl ring had a clear influence on the reactivity. Moreover, naphthalene substrate was compatible to the reaction conditions, furnishing the desired product **3n** in 61% yield.

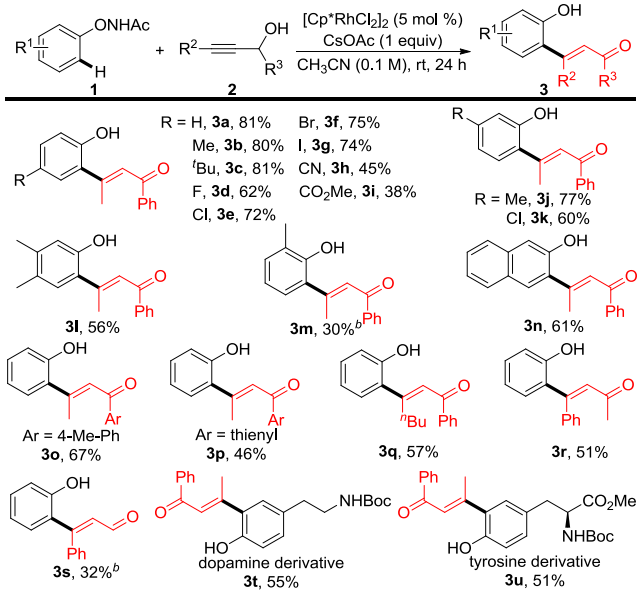

Scheme 3. Scope of Substrates for the Synthesis of Chalcones. Reaction conditions: **1** (0.2 mmol), **2** (0.4 mmol), $[Cp^*RhCl_2]_2$ (5 mol %) and CsOAc (1 equiv) in CH_3CN (0.1 M) at room temperature for 24 h under air; isolated yields were reported. [b]DCM was used as the solvent instead of CH_3CN.

Subsequently, the scope of propargyl alcohols for the synthesis of chalcones was explored. The results demonstrated that aryl (**3o**), thienyl (**3p**) and alkyl groups (**3q** and **3r**) could be all well tolerated for this transformation, affording the corresponding chalcone derivatives in moderate yields. Interestingly, 3-phenylprop-2-yn-1-ol also reacted smoothly, leading to the desired *ortho*-hydroxylphenyl-substituted phenylacrylaldehyde product **3s**. Considering the mild reaction conditions, excellent regioselectivity and good functional group tolerance, we were next intrigued to apply the present method for the late-stage C-H modification of complex bioactive compounds. Pleasantly, the derivatives of dopamine and L-tyrosine underwent the coupling with **2a** smoothly to yield the desired chalcone products **3t** and **3u** in moderate yields, which illustrated profound potentials for the rapid synthesis of drug derivatives and the construction of complex structures.

Scope of the Alternative [3+2] Annulation for the Synthesis of Benzofurans. Having established the efficient and practical approach for the synthesis of chalcone derivatives via Rh(III)-catalyzed C–H alkenylation, we next examined the substrate scope for the construction of benzofuran skeleton. As shown in Scheme 4a, various *N*-phenoxyacetamides bearing different substituents at either *para*-, *meta*- or *ortho*-position were fully tolerated, delivering the desired benzofurans in moderate to good yields (**4a-p**). Notably, trifluoromethyl- and ester-substituted *N*-phenoxyacetamides seemed to be less reactive, affording the desired benzofurans in relatively low yields (**4i** and **4j**). The result implied that the electrical property of the substituent might be crucial for determining the reaction outcome. No obvious difference on the yield was observed in terms of the substituted position on phenyl ring, which fully testified that this transformation had a broad substrate scope. Remarkably, the reaction also showed good compatibility with several natural products or drug derivatives such as dopamine, L-tyrosine and estrone skeletons, providing the corresponding benzofurans as new analogs of such structures (**4q-s**).

To better probe the versatility of this protocol for the chemoselective synthesis of benzofurans, a diverse array of propargyl alcohols were then examined under the standard conditions (Scheme 4b). In general, the reaction was compatible with various 1-arylpropargyl alcohols regardless of the electrical property of the substituent on the phenyl ring (**5a-c**). Notably, thienyl- and furyl-substituted propargyl alcohols were also good reactants for this transformation, giving the corresponding products **5d** and **5e** in good yields. Moreover, we were pleased to find that long-chain alkyl- and cycloalkyl-substituted propargyl alcohols readily participated in the [3+2] annulation, furnishing the desired benzofuran procducts **5f** and **5g** in 74% and 65% yields, respectively. Besides the 1-aryl substituted propargyl alcohols, 4-phenylbut-3-yn-2-ol was also found to be a productive substrate for this transformation, thus delivering the desired **5h** in a moderate yield. It is necessary to note that terminal propargyl alcohols (R^2 = H) were not tolerated under our conditions for the synthesis of either chalcones or benzofurans.

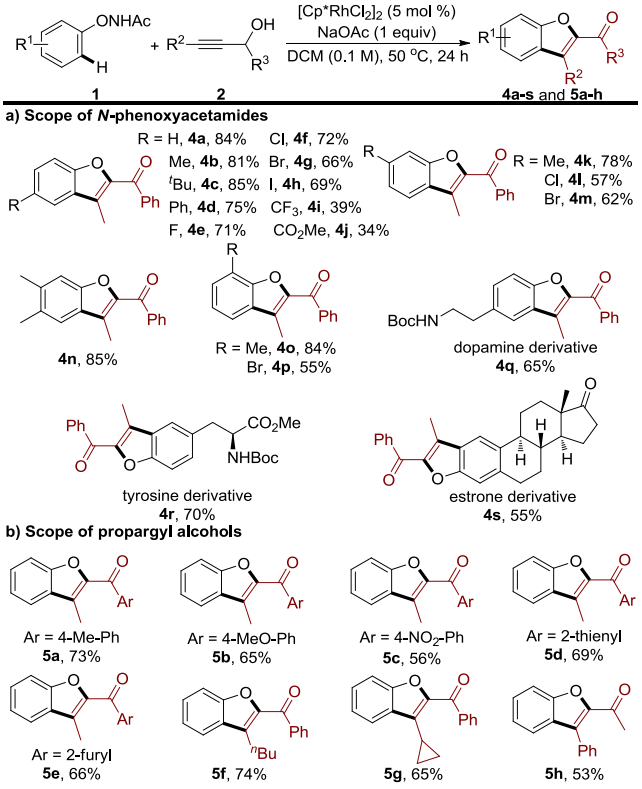

Scheme 4. Scope of Substrates for the Synthesis of Benzofurans. Reaction conditions: **1** (0.2 mmol), **2** (0.3 mmol), [Cp*RhCl2]2 (5 mol %) and NaOAc (1 equiv) in DCM (0.1 M) at 50 °C for 24 h under air; isolated yields were reported.

Mechanistic Studies. Given the novel and distinctive reaction modes enabled by the synergetic dual DGs-directed strategy and the tunable selectivity controlled by the solvent, we were next intrigued to design a set of mechanistic experiments including the experimental investigations as well as the density functional theory (DFT) studies to figure out the reaction mechanism, in particular, to clarify the role of the hydroxyl group and the origin of the chemoselectivity uniquely controlled by the solvent.

Experimental investigations to probe the reaction mechanism. To gain a better mechanistic understanding, a series of experimental investigations were first carried out (Scheme 5). Control experiments between **1a** and but-1-yn-1-ylbenzene **2k** resulted in the *ortho*-hydroxylphenyl-substituted enamide **6** and benzofuran **7** with the contrary regioselectivities compared with propargyl alcohols (Scheme 5a). These results revealed that the hydroxyl group in propargyl alcohol was indispensable for tuning the site- and regioselectivity of these approaches, and its introduction probably led to the totally reversal of the regioselectivity and different pathways to form unprecedented novel skeletons.[18] In addition, compound **8** was prepared and subjected to the Rh(III)-catalyzed [3+2] an-

nulation conditions (Scheme 5b). The result displayed that 85% of **8** was recovered and only trace product **4a** was observed, thus ruling out the presumption that the benzofuran product **4a** was derived from the alcohol precursor. Another coupling reaction of **1a** with **2a** under N_2 atmosphere resulted in the formation of (3-methyl-2,3-dihydrobenzofuran-2-yl)(phenyl)methanone intermediate, which could be easily converted into the final benzofuran product **4a** in 78% yield, verifying that **4a** was generated by further oxidation of the dihydrobenzofuran precursor. Further control experiments showed that the addition of methanol could switch the selectivity from [3+2] annulation to *ortho*-alkenylation gradually; to the end, the cyclization pathway could be totally prevented in the presence of 30% of methanol (Scheme 5c). The results exposed an obvious solvent effect that existed in these parallel experiments, and also suggested that the introduction of methanol was detrimental to the formation of the cyclization product, probably due to the protonation effect.

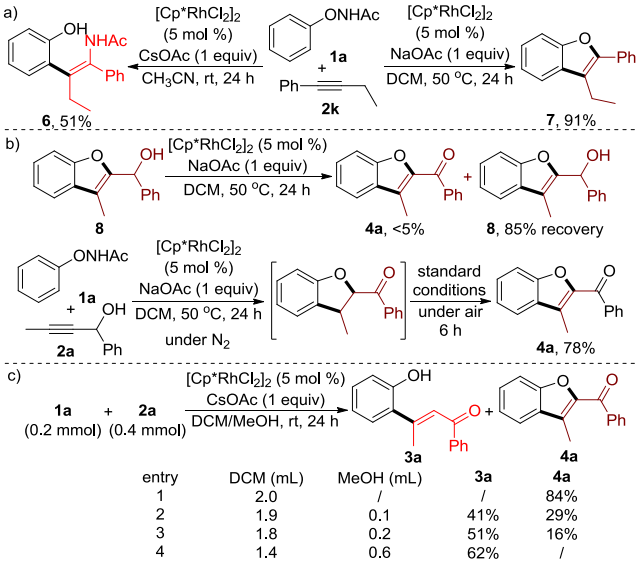

entry	DCM (mL)	MeOH (mL)	3a	4a
1	2.0	/	/	84%
2	1.9	0.1	41%	29%
3	1.8	0.2	51%	16%
4	1.4	0.6	62%	/

Scheme 5. Control Experiments

Deuterium-labeling experiments were next conducted to define the reversibility of the C–H activation process. As shown in Scheme 6a, no deuterium incorporation was observed in the recovered starting material **1a** under both conditions. Moreover, both chalcone product **3a** and benzofuran derivative **4a** could be obtained smoothly in the presence of deuterated methanol and showed no obvious deuterium incorporation at the *ortho*-position of the DG. These results indicated that the C–H metalation step was irreversible.[19] Besides, approximately 38% deuteration at the alkenyl moiety of **3a** was detected, suggesting that an active hydrogen transfer might be involved in the *ortho*-alkenylaition. Furthermore, the primary KIE values of the two divergent transformations were determined to be 1.73 and 1.34 from the independent, side-by-side experiments by measuring the initial rates of different reactions using **1a** and [D]5-**1a** as the substrates under standard conditions, implying that the C–H cleavage process might be not involved in the rate-determining step (Scheme 6b). Finally, the effort to capture the potent intermediate was achieved by treating **1a** with stoichiometric amount of [Cp*RhCl2]2 to give the desired five-membered rhodacycle complex **A** (Scheme 6c). The following coupling of rhodacycle **A** with **2a** facilely conversed into the final chalcone and benzofuran products, which provided adequate evidence to support the two C–H activation processes involving the formation of the five-membered rhodacycle **A** as the active intermediate.

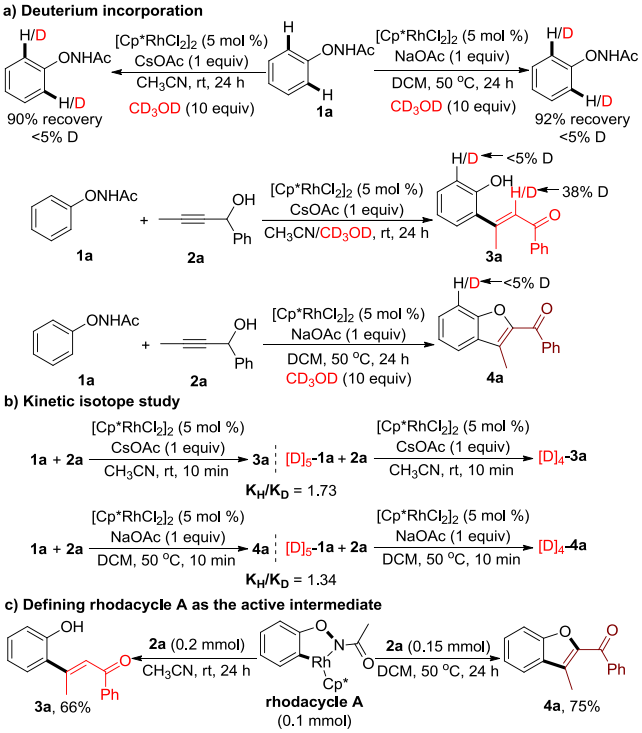

Scheme 6. Experimental Investigations

Computational studies to further uncover the reaction mechanism. To elucidate our experimental results and further cast light on details of the mechanism, computational studies were performed with density functional theory (DFT) calculations. Briefly, all the structures were optimized at the M06 level[20] in experimental solvents (DCM and methanol, respectively) to further reveal: 1) the origin of the chemoselectivity; 2) why the introduction of the hydroxyl group into the alkyne has a unique property for controlling the regioselectivity? 3) how the solvent uniquely switches the reaction outcome for the tunable synthesis of benzofurans and chalcones, respectively?

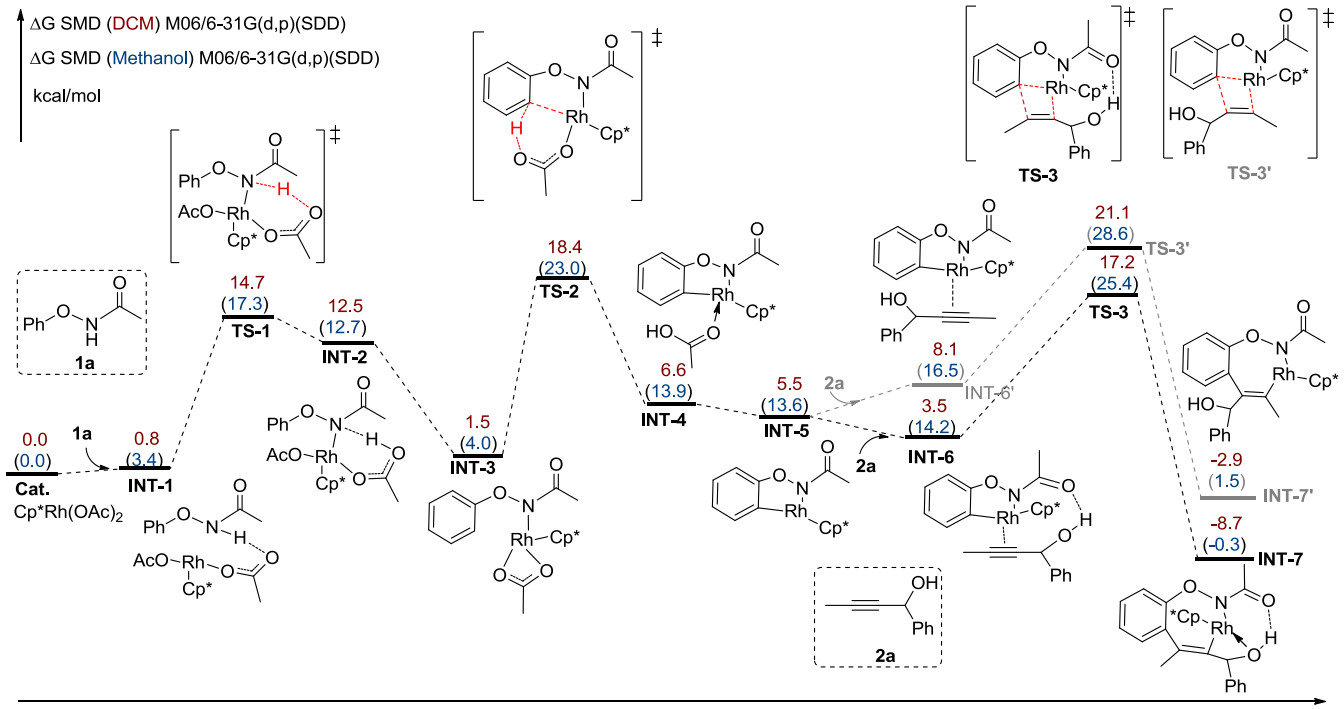

Figure 1. Computed Gibbs free energy changes of the reaction pathways for N–H deprotonation, C–H activation, and migratory insertion of propargyl alcohols in DCM (in methanol).

To address these issues, the proposed mechanism was divided into 4 key steps: N–H deprotonation, C–H activation, migratory insertion of propargyl alcohols, and the tunable formation for the products including the solvent effect for controlling such chemoselectivity. To the end, our results revealed two novel favorable mechanisms that was significantly different from that of the reported computational investigations,[21] in which the O–NHAc part was employed as the ODG. Therefore, the present DFT results provide insights into the mechanistic understandings for future development of synergistic dual DGs-directed C–H functionalization reactions.

N–H deprotonation, C–H activation, and migratory insertion of propargyl alcohols. Figure 1 shows the computational results for the formation of a seven-membered rhodacycle in both DCM and methanol solvent model. The complex Cp*Rh(OAc)2 (**Cat.**) was selected as the starting point. With DCM being the solvent, it is found that both of the N–H and C–H activation occur via a concerted metalation-deprotonation (CMD) mechanism,[22] through transition states **TS-1** ($G^{\neq}$ = 14.7 kcal/mol) and **TS-2** ($G^{\neq}$ = 18.4 kcal/mol), respectively. Thereafter, the regioselective insertion of the alkyne part proceeds via **TS-3** ($G^{\neq}$ = 17.2 kcal/mol), leading to the seven-membered rhodacycle intermediate **INT-7** with a free energy of -8.7 kcal/mol. A similar reaction pathway proceeds with a higher energy profile (values in the brackets) in methanol than that in DCM, which is consistent with the previous reported similar Rh(III)-catalyzed system.[21a,23]

By analyzing the data from Figure 1, the regioselectivity in migratory insertion of propargyl alcohols is worth noting. Our calculations showed that: a) a relatively low kinetic barrier is required for the regioselective insertion through the formation of the hydrogen bonding between dual directing groups (17.2 kcal/mol for **TS-3** vs 21.1 kcal/mol for **TS-3'**), and then, b) a stable seven-membered rhodacycle intermediate (**INT-7**) is yielded with a low free energy of -8.7 kcal/mol compared with the **INT-7'** (-2.9 kcal/mol), which should be ascribed to both the extra coordination interaction between the hydroxyl group and the catalyst metal together with the preceding formation of the hydrogen bonding. Taken together with the experimental observations, these results give a clear evidence for clarifying the remarkable role of the hydroxyl group in controlling the regioselectivity.

Chemoselective product formation pathways in DCM (via a Rh^{III}-Rh^{I}-Rh^{III} pathway). We first computed the feasibility of *β*–H elimination from the complex **INT-7** in DCM (Figure 2). The *β*–H elimination and subsequent hydrogen transfer occur via the transition state **TS-4** ($\Delta G^{\neq}$ = 10.0 kcal/mol), leading to a hydride intermediate **INT-8**. It should be emphasized that, the hydrogen transfer tunes the coordination mode of C–Rh–N moiety and converts the N–Rh covalent bond into coordination bond. Thereafter, the Rh–H bond is cleaved and the hydride is transferred to the carbon atom (via **TS-5**) with a low energy barrier, which leads to the stable intermediate **INT-9** with a free energy of -13.3 kcal/mol. Then, further hydrogen transfer proceeds via **TS-6** with a free energy barrier of 28.4 kcal/mol, yielding the Rh(I) species **INT-10**.

From **INT-10**, two possible pathways have been proposed to elaborate the chemoselectivity. In path $\mathbf{I_a}$, the

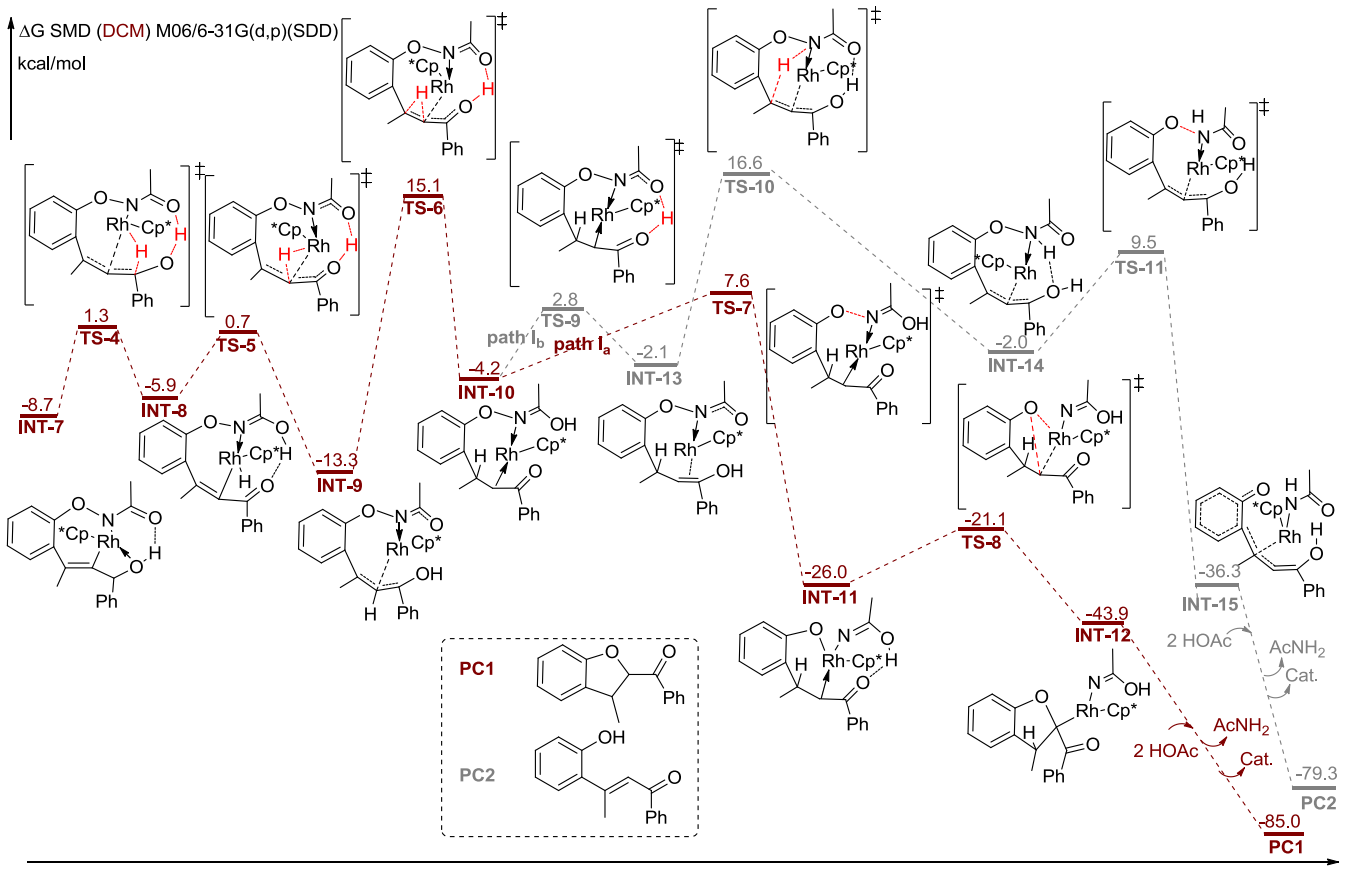

Figure 2. Computed Gibbs free energy changes of the reaction pathway in DCM.

migration of NAc from O to Rh occurs at first via a N–O cleavage transition state (**TS-7**) with a free energy of 7.6 kcal/mol, giving the Rh(III) intermediate **INT-11** in an irreversible manner. Thereafter, the species **INT-11** undergoes a reductive elimination via **TS-8**, leading to **INT-12**. Finally, the product **PC1** is generated along with the release of the active Rh(III) catalyst through the ligand exchange with HOAc. As an alternative catalytic cycle (path $\mathbf{I_b}$), the hydrogen transfer via a H-bonding transition state **TS-9** with a free energy of 2.8 kcal/mol is occurred to give the intermediate **INT-13**. Then, another hydrogen transfer via the transition state **TS-10** with a free energy of 16.6 kcal/mol is conducted to provide the intermediate **INT-14**. Thereafter, **INT-14** undergoes an intramolecular hydrogen bond dissociation via **TS-11** to generate the intermediate **INT-15**. Obviously, the highest free energy barrier of path $\mathbf{I_a}$ is 11.8 kcal/mol (from **INT-10** to **TS-7**) that is far lower than that of path $\mathbf{I_b}$ (18.7 kcal/mol, from **INT-13** to **TS-10**), suggesting that the path $\mathbf{I_a}$ is more favorable, which is agreement well with the experimental observation that the benzofuran product (**PC1**) is delivered as the major product when DCM is used as the solvent.

Besides, the highest free energy barrier (28.4 kcal/mol, from **INT-9** to **TS-6**) in the whole favorable catalytic cycle is far higher than that of the C–H activation step (18.4 kcal/mol, from **Cat.** to **TS-2**), indicating that the C-H activation is not the turn-over limiting step. The result is also in line with our kinetic isotope experiments that a small KIE value is detected.

Chemoselective product formation pathways in methanol (via a Rh^{III}-Rh^{V}-Rh^{III} pathway). Instead of the *β*–H elimination, firstly, we computed the oxidative addition to the O–N bond from complex **INT-7** in methanol (Figure 3). Initially, the migration of NAc from O to Rh occurs via the N–O cleavage transition state (**TS-12**) with a free energy of 27.1 kcal/mol, providing the intermediate **INT-16**. It can further form a more stable Rh(V) nitrenoid intermediate **INT-17** via **TS-13** with a free energy of 25.9 kcal/mol.

Following **INT-17**, two possible pathways have been proposed to elaborate the chemoselectivity. In path $\mathbf{II_a}$, **INT-17** undergoes the reductive elimination via **TS-14** with a free energy of 19.4 kcal/mol, leading to **INT-18**. Subsequently, hydrogen transfer occurs via **TS-15** and **TS-16**, respectively. Finally, the ligand exchange with HOAc generates the product and regenerates the Rh(III) catalyst. On the other hand, In path $\mathbf{II_b}$, the first hydrogen transfer of **INT-17** delivers an intermediate **INT-20** via the transition state **TS-17** with a free energy of 16.7 kcal/mol, followed by the second hydrogen transfer via the transition state **TS-18** with a low free energy of -47.9 kcal/mol to give an intermediate **INT-21**, which further approves our deuterium-labeling result that obvious deuterium incorportion is observed at the alkenyl moiety of product

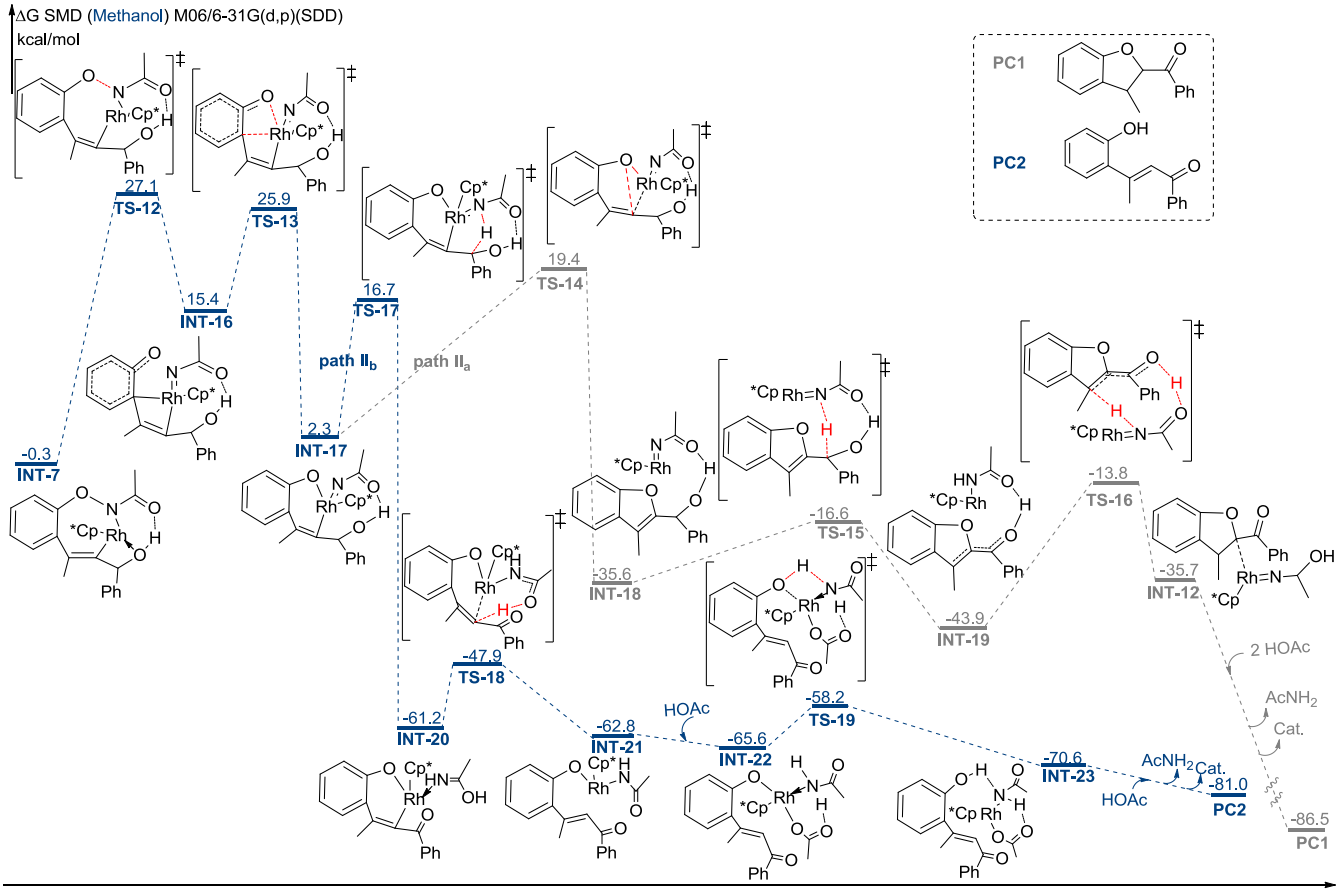

Figure 3. Computed Gibbs free energy changes of the reaction pathway in methanol.

3a. Subsequently, **INT-21** affords the intermediate **INT-22** with the addition of HOAc. Further intramolecular hydrogen transfer in **INT-22** via the transition state **TS-19** with a free energy of -58.2 kcal/mol offers the intermediate **INT-23**. Finally, the ligand exchange with HOAc generates the product with extrusion of the Rh(III) catalyst. Obviously, the free energy barrier for formation of **INT-18** in path **II$_a$** is 17.1 kcal/mol (from **INT-17** to **TS-14**) that is higher than that of path **II$_b$** (14.4 kcal/mol, from **INT-17** to **TS-17**), suggesting that the path **II$_b$** is more favorable, which is agreement well with the experimental observation that the chalcone derivative (**PC2**) presents as the preferential product with methanol being the solvent. Moreover, our computational results show that, even if the **INT-18** is formed, it is still difficult to yield the **PC1** via **TS-16** due to the existence of a higher barrier (more than 30.0 kcal/mol, from **INT-19** to **TS-16**), which further validates our experimental observation that compound **8** cannot be transformed into the corresponding benzofuran product under the current Rh(III)-catalyzed reaction conditions.

Moreover, the highest free energy barrier (27.4 kcal/mol, from **INT-7** to **TS-12**) in the whole favorable catalytic cycle pathway is higher than that of the C–H activation step (23.0 kcal/mol, from **Cat.** to **TS-2**), revealing that the N–O cleavage process rather than the C–H activation step is the rate-determining step, which is consistent with the observed small experimental KIE value in the preceding C–H cleavage process.

Tunable chemoselectivity controlled by the solvent. To better expose the solvent effect in determining the chemoselectivity, an overall comparison for the changes of the free energy in different solvents was investigated by using the representative DCM and methanol as the media model.[24]

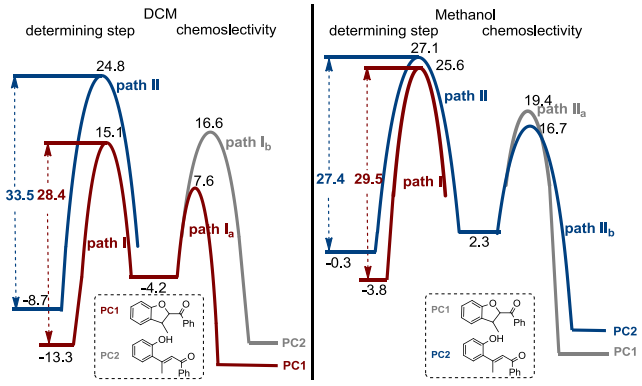

Figure 4. An overall comparison for the changes of the free energy in different solvents in determining the reactivity and chemoselectivity.

As summarized in Figure 4, our calculated results show that: a) the favorable pathway is path **I** in DCM, in which the rate-determining step barrier of 28.4 kcal/mol is sig-

nificantly lower than that of 33.5 kcal/mol in path **II**, b) in contrast, in methanol the favorable pathway is path **II** since the rate-determining step barrier of 27.4 kcal/mol is lower than that of 29.5 kcal/mol in path **I**, c) from path **I**, the path $\mathbf{I_a}$ is adopted preferentially over the path $\mathbf{I_b}$, due to the involvement of lower free energy barrier (11.8 kcal/mol vs 20.8 kcal/mol), and however, d) following path **II**, the path $\mathbf{II_b}$ is prior to the path $\mathbf{II_a}$ since a lower free energy barrier of 14.4 kcal/mol (17.4 kcal/mol for path $\mathbf{II_a}$) was involved in path $\mathbf{II_b}$.

We further calculated the electrostatic potential surfaces of the transition states (**TS-12**) for the determining step (N-O bond cleavage step) in path **II** as well as their pre-intermediate (**INT-7**) in both solvents (DCM and MeOH, respectively, see Figure S3 in the Supporting Information for details). In **INT-7**, the electron densities of the N-O bond are almost the same in both solvents, however, higher charge dispersion in **TS-12** is observed in MeOH than that in DCM. The obvious charge dispersion change indicates that the high-polar solvent decrease the barrier of **TS-12**, thus making the path **II** become a more favorable pathway in MeOH (different from that of path **I** in DCM), which leads to the chemoselective products.

Based on these, we can conclude that the low-polar solvents such as DCM favors the *β*–H elimination/hydrogen transfer/oxidative addition/C–O bond reductive elimination pathway (path $\mathbf{I\text{-}I_a}$, via a Rh^{III}-Rh^{I}-Rh^{III} pathway), leading to the chemoselective synthesis of benzofuran product via a [3 + 2] annulation. However, the high-polar solvents such as methanol prefers to follow the oxidative addition/*β*–H elimination/hydrogen transfer/protonolysis pathway (path $\mathbf{II\text{-}II_b}$, via a Rh^{III}-Rh^{V}-Rh^{III} pathway), resulting in the chemoselective construction of chalcone product via the *ortho*-alkenylation, which goes well with the experimental observations.

Mechanistic proposal. On the basis of these computational and experimental studies, a plausible mechanism involving the synergistic O–NHAc part and hydroxyl group-directed regioselective C–H activation process is proposed (Scheme 7). Initially, the active Cp*Rh(OAc)2 is generated through anion exchange, followed by facile irreversible *ortho*-rhodation via a CMD mechanism to deliver the five-membered rhodacycle intermediate **A** (**INT-5**). Subsequent regioselective migratory insertion of the alkyne moiety of **2a** into the Rh–C bond of **A** forms the seven-membered intermediate **B** (**INT-7**), which is stabilized by the Rh–O coordination and the hydrogen bonding interaction. Thereafter, there are two distinct reaction pathways depending on the polarity of the solvent. For the low-polar solvents (*e.g.* DCM and DCE), a plausible β–H elimination and subsequent hydrogen transfer are involved to afford the intermediate **E** (**INT-9**). Further intramolecular hydrogen transfer occurs that is used as the rate-determining step with a free energy barrier of 28.4 kcal/mol (from **INT-9** to **TS-10**) to generate the Rh(I) intermediate **F** (**INT-10**), which then undergoes sequential oxidative addition/C–O bond reductive elimination to provide the cyclized dihydrobenzofuran skeleton **H** (**PC1**) along with the release of the active Rh(III) catalyst. Further oxidation of **H** under air[25] provides the final benzofuran product **4a**. Alternatively, **B** undergoes a turnover-limiting oxidative addition process (27.4 kcal/mol, from **INT-7** to **TS-12**) in the high-polar solvents (*e.g.* methanol and CH_3CN) to give the Rh(V) species **C** (**INT-17**). Further *β*–H elimination of **C** and then hydrogen transfer yield an intermediate **D** (**INT-21**), followed by the protonolysis of **D** with the aid of HOAc to deliver the chalcone derivative **3a** and regenerate the active Rh(III) catalyst.

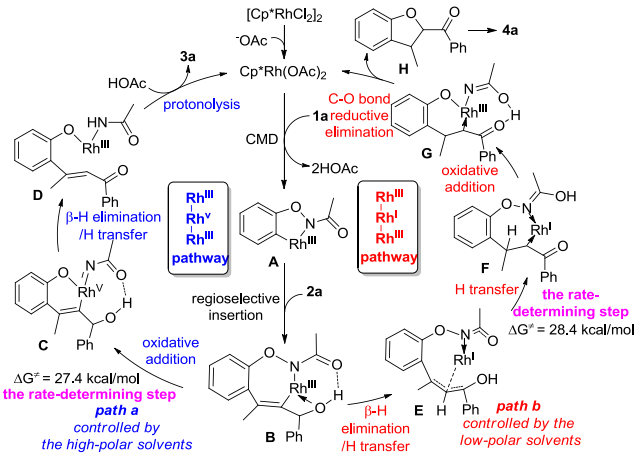

Scheme 7. Summary of the Proposed Mechanism

CONCLUSION

In summary, by employing the synergetic dual DGs-directed strategy, we have developed for the first time the mild rhodium(III)-catalyzed and solvent-controlled redox-neutral C–H functionalization of *N*-phenoxyacetamides with new type of primary or secondary chelating propargyl alcohols for the divergent synthesis of chalcone and benzofuran derivatives with exclusive regioselectivity, tunable chemoselectivity, and good substrate/functional group compatibility. The role of the hydroxyl group, the distinct catalytic mode, the rate-determining step, the origin of the chemoselectivity, as well as two solvent-controlled chemoselective reaction pathways are rationally clarified by a combined experimental and DFT study. Taken together, our present results not only give a remarkable and meaningful expansion in the area of TM-catalyzed and O–NHAc-assisted C–H activations but also provide a rational basis for future development of synergistic dual DGs-directed C–H functionalization reactions. Furthermore, recognizing the great importance of the obtained product skeletons in organic synthesis, medicinal chemistry and materials science, we believe that the two versatile transformations should have attractive prospects for the synthetic utility. Further expansion of this synergetic dual DGs-directed strategy to develop the more diverse transformations is in progress.

ASSOCIATED CONTENT

Supporting Information. Experimental procedures, characterization of products, computational details and copies of ^{1}H and ^{13}C spectra are provided. This material is available free of charge via the Internet at http://pubs.acs.org.

AUTHOR INFORMATION

Corresponding Author
*zhouzhi@gzhmu.edu.cn
*gaoh9@gzhmu.edu.cn
*yiwei@gzhmu.edu.cn

Notes
The authors declare no competing financial interest.

ACKNOWLEDGMENT

We thank NSFC (81502909 and 21877020), Guangdong Natural Science Funds for Distinguished Young Scholar (2017A030306031), Natural Science Foundation Research Team of Guangdong Province (2018B030312001) and Natural Science Foundation of Guangdong Province (2017A030313058) for financial support on this study.

REFERENCES

(1) For recent selected reviews, see: (a) Baudoin, O. Ring Construction by Palladium(0)-Catalyzed C(sp^3)-H Activation. *Acc. Chem. Res.* **2017**, *50*, 1114-1123. (b) Wei, Y.; Hu, P.; Zhang, M.; Su, W. Metal-Catalyzed Decarboxylative C-H Functionalization. *Chem. Rev.* **2017**, *117*, 8864-8907. (c) He, J.; Wasa, M.; Chan, K. S. L.; Shao, Q.; Yu, J.-Q. Palladium-Catalyzed Transformations of Alkyl C-H Bonds. *Chem. Rev.* **2017**, *117*, 8754-8786. (d) Park, Y.; Kim, Y.; Chang, S. Transition Metal-Catalyzed C-H Amination: Scope, Mechanism, and Applications. *Chem. Rev.* **2017**, *117*, 9247-9301. (e) Gandeepan, P.; Ackermann, L. Transient Directing Groups for Transformative C–H Activation by Synergistic Metal Catalysis. *Chem* **2018**, *4*, 199-222.

(2) For representative reviews, see: (a) Lewis, J. C.; Bergman, R. G.; Ellman, J. A. Direct Functionalization of Nitrogen Heterocycles via Rh-Catalyzed C-H Bond Activation. *Acc. Chem. Res.* **2008**, *41*, 1013-1025. (b) Chen, X.; Engle, K. M.; Wang, D. H.; Yu, J.-Q. Palladium(II)-Catalyzed C-H Activation/C-C Cross-Coupling Reactions: Versatility and Practicality. *Angew. Chem., Int. Ed.* **2009**, *48*, 5094-5115. (c) Colby, D. A.; Bergman, R. G.; Ellman, J. A. Rhodium-Catalyzed C-C Bond Formation via Heteroatom-Directed C-H Bond Activation. *Chem. Rev.* **2010**, *110*, 624-655. (d) Cho, S. H.; Kim, J. Y.; Kwak, J.; Chang, S. Recent Advances in the Transition Metal-Catalyzed Twofold Oxidative C-H Bond Activation Strategy for C-C and C-N Bond Formation. *Chem. Soc. Rev.* **2011**, *40*, 5068-5083. (e) Song, G.; Wang, F.; Li, X. C-C, C-O and C-N Bond Formation via Rhodium(III)-Catalyzed Oxidative C-H Activation. *Chem. Soc. Rev.* **2012**, *41*, 3651-3678. (f) Li, B.-J.; Shi, Z.-J. From C(sp^2)-H to C(sp^3)-H: Systematic Studies on Transition Metal-Catalyzed Oxidative C-C Formation. *Chem. Soc. Rev.* **2012**, *41*, 5588-5598. (g) Hartwig, J. F. Borylation and Silylation of C-H Bonds: a Platform for Diverse C-H Bond Functionalizations. *Acc. Chem. Res.* **2012**, *45*, 864-873. (h) Wencel-Delord, J.; Glorius, F. C-H Bond Activation Enables the Rapid Construction and Late-Stage Diversification of Functional Molecules. *Nat. Chem.* **2013**, *5*, 369-375. (i) Ackermann, L. Carboxylate-Assisted Ruthenium-Catalyzed Alkyne Annulations by C-H/Het-H Bond Functionalizations. *Acc. Chem. Res.* **2014**, *47*, 281-295. (j) Kuhl, N.; Schröder, N.; Glorius, F. Formal S_N-Type Reactions in Rhodium(III)-Catalyzed C-H Bond Activation. *Adv. Synth. Catal.* **2014**, *356*, 1443-1460. (k) Shin, K.; Kim, H.; Chang, S. Transition-Metal-Catalyzed C-N Bond Forming Reactions Using Organic Azides as the Nitrogen Source: a Journey for the Mild and Versatile C-H Amination. *Acc. Chem. Res.* **2015**, *48*, 1040-1052. (l) Zhu, R. Y.; Farmer, M. E.; Chen, Y. Q.; Yu, J. Q. A Simple and Versatile Amide Directing Group for C-H Functionalizations. *Angew. Chem., Int. Ed.* **2016**, *55*, 10578-10599. (m) Mishra, N. K.; Sharma, S.; Park, J.; Han, S.; Kim, I. S. Recent Advances in Catalytic C(sp^2)–H Allylation Reactions. *ACS Catal.* **2017**, *7*, 2821-2847. (n) Ackermann, L. Carboxylate-Assisted Transition-Metal-Catalyzed C-H Bond Functionalizations: Mechanism and Scope. *Chem. Rev.* **2011**, *111*, 1315-1345. (o) Gensch, T.; Hopkinson, M. N.; Glorius, F.; Wencel-Delord, J. Mild Metal-Catalyzed C-H Activation: Examples and Concepts. *Chem. Soc. Rev.* **2016**, *45*, 2900-2936. (p) Huang, H.; Ji, X.; Wu, W.; Jiang, H. Transition Metal-Catalyzed C-H Functionalization of *N*-Oxyenamine Internal Oxidants. *Chem. Soc. Rev.* **2015**, *44*, 1155-1171. (q) Ping, L.; Chung, D. S.; Bouffard, J.; Lee, S.-G. Transition Metal-Catalyzed Site- and Regio-Divergent C-H Bond Functionalization. *Chem. Soc. Rev.* **2017**, 46, 4299-4328. (r) Kim, D.-S.; Park, W.-J.; Jun, C.-H. Metal-Organic Cooperative Catalysis in C-H and C-C Bond Activation. *Chem. Rev.* **2017**, *117*, 8977-9015.

(3) For the latest selected examples, see: (a) Mei, R.; Sauermann, N.; Oliveira, J. C. A.; Ackermann, L. Electroremovable Traceless Hydrazides for Cobalt-Catalyzed Electro-Oxidative C-H/N-H Activation with Internal Alkynes. *J. Am. Chem. Soc.* **2018**, *140*, 7913-7921. (b) Font, M.; Cendón, B.; Seoane, A.; Mascareñas, J. L.; Gulías, M. Rhodium(III)-Catalyzed Annulation of 2-Alkenyl Anilides with Alkynes through C-H Activation: Direct Access to 2-Substituted Indolines. *Angew. Chem., Int. Ed.* **2018**, *57*, 8255-8259. (c) Lu, Q.; Mondal, S.; Cembellín, S.; Glorius, F. Mn(I)/Ag(I) Relay Catalysis: Traceless Diazo-Assisted C(sp^2)-H/C(sp^3)-H Coupling to beta-(Hetero)Aryl/Alkenyl Ketones. *Angew. Chem., Int. Ed.* **2018**, *57*, 10732-10736. (d) Zhou, X.; Xia, J.; Zheng, G.; Kong, L.; Li, X. Divergent Coupling of Anilines and Enones by Integration of C-H Activation and Transfer Hydrogenation. *Angew. Chem., Int. Ed.* **2018**, *57*, 6681-6685. (e) Qiu, Y.; Tian, C.; Massignan, L.; Rogge, T.; Ackermann, L. Electrooxidative Ruthenium-Catalyzed C-H/O-H Annulation by Weak O-Coordination. *Angew. Chem., Int. Ed.* **2018**, *57*, 5818-5822. (f) Li, M.; Kwong, F. Y. Cobalt-Catalyzed Tandem C-H Activation/C-C Cleavage/C-H Cyclization of Aromatic Amides with Alkylidenecyclopropanes. *Angew. Chem., Int. Ed.* **2018**, *57*, 6512-6516. (g) Hong, S. Y.; Park, Y.; Hwang, Y.; Kim, Y. B.; Baik, M.-H.; Chang, S. Selective Formation of γ-Lactams via C-H Amidation Enabled by Tailored Iridium Catalysts. *Science* **2018**, *359*, 1016-1021. (h) Shin, K.; Park, Y.; Baik, M.-H.; Chang, S. Iridium-Catalysed Arylation of C-H Bonds Enabled by Oxidatively Induced Reductive Elimination. *Nat. Chem.*, **2018**, *10*, 218-224. (i) Halskov, K. S.; Witten, M. R.; Hoang, G. L.; Mercado, B. Q.; Ellman, J. A. Rhodium(III)-Catalyzed Imidoyl C-H Activation for Annulations to Azolopyrimidines. *Org. Lett.* **2018**, *20*, 2464-2467. (j) Su, B.; Hartwig, J. F. Ir-Catalyzed, Silyl-Directed, peri-Borylation of C-H Bonds in Fused Polycyclic Arenes and Heteroarenes. *Angew. Chem., Int. Ed.* **2018**, *57*, 10163-10167. (k) Lu, H.; Fan, Z.; Xiong, C.; Zhang, A. Highly Stereoselective Assembly of Polycyclic Molecules from 1,6-Enynes Triggered by Rhodium(III)-Catalyzed C-H Activation. *Org. Lett.* **2018**, *20*, 3065-3069. (l) Yu, X.; Chen, K.; Wang, Q.; Zhang, W.; Zhu, J. Synthesis of 2,5-Disubstituted Oxazoles via Cobalt(III)-Catalyzed Cross-Coupling of *N*-Pivaloyloxyamides and Alkynes. *Chem. Commun.* **2018**, *54*, 1197-1200.

(4) For recent selected reviews on C-H functionalization using bidentate chelating auxiliaries, see: (a) Rouquet, G.; Chatani, N. Catalytic Functionalization of C(sp^2)-H and C(sp^3)-H Bonds by Using Bidentate Directing Groups. *Angew. Chem., Int. Ed.* **2013**, *52*, 11726-11743. (b) Liu, J.; Chen, G.; Tan, Z. Copper-Catalyzed or -Mediated C-H Bond Functionalizations Assisted by Bidentate Directing

Groups. *Adv. Synth. Catal.* **2016**, *358*, 1174-1194. (c) Yang, X.; Shan, G.; Wang, L.; Rao, Y. Recent advances in transition metal (Pd, Ni)-catalyzed C(sp^3)H bond activation with bidentate directing groups. *Tetrahedron Lett.* **2016**, *57*, 819-836. (d) Kommagalla, Y.; Chatani, N. Cobalt(II)-Catalyzed C-H Functionalization Using an *N,N'*-Bidentate Directing Group. *Coord. Chem. Rev.* **2017**, *350*, 117-135.

(5) For selected reviews, see: (a) Daugulis, O.; Roane, J.; Tran, L. D. Bidentate, Monoanionic Auxiliary-Directed Functionalization of Carbon-Hydrogen Bonds. *Acc. Chem. Res.* **2015**, *48*, 1053-1064. (b) Misal Castro, L. C.; Chatani, N. Nickel Catalysts/*N,N'*-Bidentate Directing Groups: An Excellent Partnership in Directed C-H Activation Reactions. *Chem. Lett.* **2015**, *44*, 410-421.

(6) For selected examples, see: (a) Hao, X.-Q.; Chen, L.-J.; Ren, B.; Li, L.-Y.; Yang, X.-Y.; Gong, J.-F.; Niu, J.-L.; Song, M.-P. Copper-Mediated Direct Aryloxylation of Benzamides Assisted by an *N,O*-Bidentate Directing Group. *Org. Lett.* **2014**, *16*, 1104-1107. (b) Guan, M.; Pang, Y.; Zhang, J.; Zhao, Y. Pd-Catalyzed Sequential β-C(sp^3)-H Arylation and Intramolecular Amination of δ-C(sp^2)-H Bonds for Synthesis of Quinolinones via an *N,O*-Bidentate Directing Group. *Chem. Commun.*, **2016**, *52*, 7043-7046. (c) Li, G.; Liu, P.; Zhang, J.; Shi, D.-Q.; Zhao, Y. Palladium-Catalyzed Direct *Ortho*-Alkynylation of Arylalkylacid Derivatives at γ and δ Positions via an *N,O*-Bidentate Directing Group. *Org. Chem. Front.*, **2017**, *4*, 1931-1934.

(7) (a) Gutekunst, W. R.; Baran, P. S. Total Synthesis and Structural Revision of the Piperarborenines via Sequential Cyclobutane C-H Arylation. *J. Am. Chem. Soc.*, **2011**, *133*, 19076-19079. (b) Tran, L. D.; Daugulis, O. Nonnatural Amino Acid Synthesis by Using Carbon-Hydrogen Bond Functionalization Methodology. *Angew. Chem., Int. Ed.* **2012**, *51*, 5188-5191. (c) Parella, R.; Gopalakrishnan, B.; Babu, S. A. Auxiliary-Enabled Pd-Catalyzed Direct Arylation of Methylene C(sp^3)-H Bond of Cyclopropanes: Highly Diastereoselective Assembling of Di- and Trisubstituted Cyclopropanecarboxamides. *Org. Lett.* **2013**, *15*, 3238-3241.

(8) Lu, Q.; Greβies, S.; Cembellín, S.; Klauck, F. J. R; Daniliuc, C. G.; Glorius, F. Redox-Neutral Manganese(I)-Catalyzed C-H Activation: Traceless Directing Group Enabled Regioselective Annulation. *Angew. Chem., Int. Ed.* **2017**, *56*, 12778-12782.

(9) (a) Gong, W.; Zhou, Z.; Shi, J.; Wu, B.; Huang, B.; Yi, W. Catalyst-Controlled [3 + 2] and [4 + 2] Annulations of Oximes with Propargyl Alcohols: Divergent Access to Indenamines and Isoquinolines. *Org. Lett.* **2018**, *20*, 182-185. (b) Chen, W.; Liu, F.-X.; Gong, W.; Zhou, Z.; Gao, H.; Shi, J.; Wu, B.; Yi, W. Hydroxyl Group-Prompted and Iridium(III)-Catalyzed Regioselective C–H Annulation of *N*-phenoxyacetamides with Propargyl Alcohols. *Adv. Synth. Catal.* **2018**, *360*, 2470-2475.

(10) For selected recent examples on TM-catalyzed C-H functionalization with propargyl alcohols, see: (a) Wu, X.; Wang, B.; Zhou, Y.; Liu, H. Propargyl Alcohols as One-Carbon Synthons: Redox-Neutral Rhodium(III)-Catalyzed C-H Bond Activation for the Synthesis of Isoindolinones Bearing a Quaternary Carbon. *Org. Lett.* **2017**, *19*, 1294-1297. (b) Sen, M.; Dahiya, P.; Premkumar, J. R.; Sundararaju, B. Dehydrative Cp*Co(III)-Catalyzed C-H Bond Allenylation. *Org. Lett.* **2017**, *19*, 3699-3602. (c) Wu, X.; Wang, B.; Zhou, S.; Zhou, Y.; Liu, H. Ruthenium-Catalyzed Redox-Neutral [4+1] Annulation of Benzamides and Propargyl Alcohols via C–H Bond Activation. *ACS Catal.* **2017**, *7*, 2494-2499. (d) Wu, S.; Wu, X.; Fu, C.; Ma, S. Rhodium(III)-Catalyzed C-H Functionalization in Water for Isoindolin-1-one Synthesis. *Org. Lett.* **2018**, *20*, 2831-2834. (e) Wu, X.; Ji, H. Rhodium-Catalyzed [4+1] Cyclization via C-H Activation for the Synthesis of Divergent Heterocycles Bearing a Quaternary Carbon. *J. Org. Chem.* **2018**, *83*, 4650-4656.

(11) (a) Sahu, N. K.; Balbhadra, S. S.; Choudhary, J.; Kohli, D. V. Exploring Pharmacological Significance of Chalcone Scaffold: a Review. *Curr. Med. Chem.* **2012**, *19*, 209-225. (b) Nevagi, R. J.; Dighe, S. N.; Dighe, S. N. Biological and Medicinal Significance of Benzofuran. *Eur. J. Med. Chem.* **2015**, *97*, 561-581. (c) Zhuang, C.; Zhang, W.; Sheng, C.; Zhang, W.; Xing, C.; Miao, Z. Chalcone: A Privileged Structure in Medicinal Chemistry. *Chem. Rev.* **2017**, *117*, 7762-7810.

(12) The selected examples for TM-catalyzed and O–NHAc-directed C-H functionalizations with alkynes, see: (a) Liu, G.; Shen, Y.; Zhou, Z.; Lu, X. Rhodium(III)-Catalyzed Redox-Neutral Coupling of *N*-Phenoxyacetamides and Alkynes with Tunable Selectivity. *Angew. Chem., Int. Ed.* **2013**, *52*, 6033-6037. (b) Zhou, Z.; Liu, G.; Chen, Y.; Lu, X. Cascade Synthesis of 3-Alkylidene Dihydrobenzofuran Derivatives via Rhodium(III)-Catalyzed Redox-Neutral C-H Functionalization/Cyclization. *Org. Lett.* **2015**, *17*, 5874-5877. (c) Zhou, Z.; Liu, G.; Shen, Y.; Lu, X. Synthesis of Benzofurans via Ruthenium-Catalyzed Redox-Neutral C–H Functionalization and Reaction with Alkynes under Mild Conditions. *Org. Chem. Front.* **2014**, *1*, 1161-1165. (d) Chen, Y.; Wang, D.; Duan, P.; Ben, R.; Dai, L.; Shao, X.; Hong, M.; Zhao, J.; Huang, Y. A Multitasking Functional Group Leads to Structural Diversity Using Designer C-H Activation Reaction Cascades. *Nat. Commun.* **2014**, *5*, 4610. (e) Xie, Y. Acylation of Csp^2-H Bond with Acyl Sources Derived from Alkynes: Rh-Cu Bimetallic Catalyzed C[triple bond, length as m-dash]C Bond Cleavage. *Chem. Commun.* **2016**, *52*, 12372-12375. (f) Hu, S.; Lu, L.; Zhu, T.; Wu, Q.; Chen, Y.; Li, J. J.; Zhao, J. Rh(III)-Catalyzed *ortho*-C-H Alkynylation of *N*-Phenoxyacetamides with Hypervalent Iodine-Alkyne Reagents at Room Temperature. *Org. Biomol. Chem.* **2018**, *16*, 43-47. (g) Zhou, J.; Shi, J.; Qi, Z.; Li, X.; Xu, H. E.; Yi, W. Mild and Efficient Ir(III)-Catalyzed Direct C-H Alkynylation of *N*-Phenoxyacetamides with Terminal Alkyne. *ACS Catal.* **2015**, *5*, 6999.

(13) The selected examples for TM-catalyzed and O–NHAc-directed C-H functionalizations with alkenes, see: (a) Shen, Y.; Liu, G.; Zhou Z.; Lu, X. Rhodium(III)-Catalyzed C-H Olefination for the Synthesis of *ortho*-Alkenyl Phenols Using an Oxidizing Directing Group. *Org. Lett.* **2013**, *15*, 3366-3369. (b) Wang, X.; Lerchen, A.; Daniliuc, C. G.; Glorius, F. Efficient Synthesis of Arylated Furans by a Sequential Rh-Catalyzed Arylation and Cycloisomerization of Cyclopropenes. *Angew. Chem., Int. Ed.* **2018**, *57*, 1712-1716. (c) Wang, X.; Lerchen, A.; Gensch, T.; Knecht, T.; Daniliuc, C. G.; Glorius, F. Combination of Cp^*Rh^{III}-Catalyzed C-H Activation and a Wagner-Meerwein-Type Rearrangement. *Angew. Chem., Int. Ed.* **2017**, *56*, 1381-1384. (d) Lerchen, A.; Knecht, T.; Daniliuc, C. G.; Glorius, F. Unnatural Amino Acid Synthesis Enabled by the Regioselective Cobalt(III)-Catalyzed Intermolecular Carboamination of Alkenes. *Angew. Chem., Int. Ed.* **2016**, *55*, 15166-15170. (e) Zhang, H.; Wang, K.; Wang, B.; Yi, H.; Hu, F.; Li, C.; Zhang, Y.; Wang, J. Rhodium(III)-Catalyzed Transannulation of Cyclopropenes with *N*-Phenoxyacetamides through C-H Activation. *Angew. Chem., Int. Ed.* **2014**, *53*, 13234-13238. (f) Hu, Z.; Tong, X.; Liu, G. Rhodium(III) Catalyzed Carboamination of Alkenes Triggered by C-H Activation of *N*-Phenoxyacetamides under Redox-Neutral Conditions. *Org. Lett.* **2016**, *18*, 1702-1705. (g) Piou, T.; Rovis, T. Rhodium-Vatalysed *syn*-Carboamination of Alkenes via a Transient Directing Group. *Nature* **2015**, *527*, 86-90. (h) Prakash, S.; Muralirajan, K.; Cheng, C.-H. Rh-Catalyzed Oxidizing Group-Directed *ortho* C-H Vinylation of Arenes by

Vinylstannanes. *Chem. Commun.* **2015**, *51*, 13362-13364. (i) Li, Y.; Tang, Y.; He, X.; Shi, D.; Wu, J.; Xu, S. Rhodium(III)-Catalyzed Annulative Carbooxygenation of 1,1-Disubstituted Alkenes Triggered by C-H Activation. *Chem.-Eur. J.* **2017**, *23*, 7453-7457.

(14) The selected examples for TM-catalyzed and O–NHAc-directed C-H functionalizations with diazo compounds, see: (a) Hu, F.; Xia, Y.;Ye, F.; Liu, Z.; Ma, C.; Zhang Y.; Wang, J. Rhodium(III)-catalyzed ortho alkenylation of N-phenoxyacetamides with N-tosylhydrazones or diazoesters through C-H activation. *Angew. Chem., Int. Ed.* **2014**, *53*, 1364-1367. (b) Hu, Z.; Liu, G. Rhodium(III) - Catalyzed Cascade Redox - Neutral C – H Functionalization and Aromatization: Synthesis of Unsymmetrical ortho - Biphenols. *Adv. Synth. Catal.* **2017**, *359*, 1643-1648. (c) Wu, Y.; Chen, Z.; Yang, Y.; Zhu, W.; Zhou, B. Rh(III)-Catalyzed Redox-Neutral Unsymmetrical C-H Alkylation and Amidation Reactions of N-Phenoxyacetamides. *J. Am. Chem. Soc.* **2018**, *140*, 42-45. (d) Zhou, J.; Shi, J.; Liu, X.; Jia, J.; Song, H.; Xu, H. E.; Yi, W. Rh(III)-Catalyzed and Alcohol-Involved Carbenoid C-H Insertion into *N*-Phenoxyacetamides Using α-Diazomalonates. *Chem. Commun.* **2015**, *51*, 5868-5871.

(15) For representative examples, see: (a) Wang, X.; Gensch, T.; Lerchen, A.; Daniliuc, C. G.; Glorius, F. Cp*Rh(III)/Bicyclic Olefin Cocatalyzed C-H Bond Amidation by Intramolecular Amide Transfer. *J. Am. Chem. Soc.* **2017**, *139*, 6506-6512. (b) Li, B.; Zhou, L.; Cheng, H.; Huang, Q.; Lan, J.; Zhou, L.; You, J. Dual-Emissive 2-(2'-Hydroxyphenyl)oxazoles for High Performance Organic Electroluminescent Devices: Discovery of a New Equilibrium of Excited State Intramolecular Proton Transfer with a Reverse Intersystem Crossing Process. *Chem. Sci.* **2018**, *9*, 1213-1220. (c) Li, B.; Tang, G.; Zhou, L.; Wu, D.; Lan, J.; Zhou, L.; Lu, Z.; You, J. Unexpected Sole Enol-Form Emission of 2 - (2'-Hydroxyphenyl)oxazoles for Highly Efficient Deep-Blue-Emitting Organic Electroluminescent Devices. *Adv. Funct. Mater.* **2017**, *27*, 1605245. (d) Li, B.; Lan, J.; Wu, D.; You, J. Rhodium(III)-Catalyzed *ortho*-Heteroarylation of Phenols through Internal Oxidative C-H Activation: Rapid Screening of Single-Molecular White-Light-Emitting Materials. *Angew. Chem., Int. Ed.* **2015**, *54*, 14008-14012. (e) Wu, Q.; Chen, Y.; Yan, D.; Zhang, M.; Lu, Y.; Sun, W.-Y.; Zhao, J. Unified Synthesis of mono/bis-Arylated Phenols via Rh^{III}-Catalyzed Dehydrogenative Coupling. *Chem. Sci.* **2017**, *8*, 169-173. (f) Wu, Q.; Yan, D.; Chen, Y.; Wang, T.; Xiong, F.; Wei, W.; Lu, Y.; Sun, W.-Y.; Li, J. J.; Zhao, J. A Redox-Neutral Catechol Synthesis. *Nat. Commun.* **2017**, *8*, 14227. (g) Duan, P.; Lan, X.; Chen, Y.; Qian, S.-S.; Li, J. J.; Lu, L.; Lu, Y.; Chen, B.; Hong, M.; Zhao, J. Rhodium(III)-Catalyzed C-H Activation/[4+3] Annulation of *N*-Phenoxyacetamides and α,β-Unsaturated Aldehydes: an Efficient Route to 1,2-Oxazepines at Room Temperature. *Chem. Commun.* **2014**, *50*, 12135-12138. (h) Duan, P.; Yang, Y.; Ben, R.; Yan, Y.; Dai, L.; Hong, M.; Wu, Y.-D.; Wang, D.; Zhang X.; Zhao, J. Palladium-Catalyzed Benzo[d]isoxazole Synthesis by C–H Activation/[4 + 1] Annulation. *Chem. Sci.* **2014**, *5*, 1574-1578. (i) Wang, H.; Wang, B.; Li, B. Synthesis of 3-Arylbenzofuran-2-ylphosphines via Rhodium-Catalyzed Redox-Neutral C-H Activation and Their Applications in Palladium-Catalyzed Cross-Coupling of Aryl Chlorides. *J. Org. Chem.* **2017**, *82*, 9560-9569. (j) Zhang, Y.; He, Y.; Li, L.; Ji, M.; Li, X-Z.; Zhu, G. Synthesis of Polyaryl-Substituted Olefins via a Rh(III)-Catalyzed One-Pot Reaction Using *N*-Phenoxyacetamides, Ketones, and Hydrazines. *J. Org. Chem.* **2018**, *83*, 2898-2903.

(16) For detailed optimization studies, see Table S1 and S2 in the Supporting Information.

(17) (a) Hummel, J. R.; Boerth, J. A.; Ellman, J. A. Transition-Metal-Catalyzed C-H Bond Addition to Carbonyls, Imines, and Related Polarized π Bonds. *Chem. Rev.* **2017**, *117*, 9163-9227. (b) Xia, Y.; Qiu, D.; Wang, J. Transition-Metal-Catalyzed Cross-Couplings through Carbene Migratory Insertion. *Chem Rev.* **2017**, *117*, 13810-13889. (c) Kim, H.; Chang, S. The Use of Ammonia as an Ultimate Amino Source in the Transition Metal-Catalyzed C-H Amination. *Acc. Chem. Res.*, **2017**, *50*, 482-486. (d) Moselage, M.; Li, J.; Ackermann, L. Cobalt-Catalyzed C–H Activation. *ACS Catal.* **2016**, *6*, 498-525.

(18) Other control experiments with 1-phenyl-2-butyne substrate were conducted and resulted in the formation of a mixture of benzofurans containing two regio isomers. For details, see the Supporting Information.

(19) (a) Ferrer Flegeau, E.; Bruneau, C.; Dixneuf, P. H.; Anny Jutand, A. Autocatalysis for C–H Bond Activation by Ruthenium(II) Complexes in Catalytic Arylation of Functional Arenes. *J. Am. Chem. Soc.* **2011**, *133*, 10161–10170. (b) Ackermann, L.; Wang, L.; Wolfram, R.; Lygin, A. V. Ruthenium-Catalyzed Oxidative C-H Alkenylations of Anilides and Benzamides in Water. *Org Lett.* **2012**, *14*, 728-731. (c) Hyster, T. K.; Rovis, T. Rhodium-Catalyzed Oxidative Cycloaddition of Benzamides and Alkynes via C-H/N-H Activation *J. Am. Chem. Soc.* **2010**, *132*, 10565-10569. (d) Guimond, N.; Gorelsky, S. I.; Fagnou, K. Rhodium(III)-Catalyzed Heterocycle Synthesis Using an Internal Oxidant: Improved Reactivity and Mechanistic Studies. *J. Am. Chem. Soc.* **2011**, *133*, 6449-6457.

(20) For details, see the Supporting Information.

(21) (a) Yang, Y.-F.; Houk, K. N.; Wu, Y.-D. Computational Exploration of Rh(III)/Rh(V) and Rh(III)/Rh(I) Catalysis in Rhodium(III)-Catalyzed C-H Activation Reactions of *N*-Phenoxyacetamides with Alkynes. *J. Am. Chem. Soc.* **2016**, *138*, 6861-6868. (b) Li, J.; Qiu, Z. DFT Studies on the Mechanism of the Rhodium(III)-Catalyzed C-H Activation of *N*-Phenoxyacetamide. *J. Org. Chem.* **2015**, *80*, 10686-10693. (c) Chen, J.; Guo, W.; Xia, Y. Computational Revisit to the β-Carbon Elimination Step in Rh(III)-Catalyzed C-H Activation/Cycloaddition Reactions of *N*-Phenoxyacetamide and Cyclopropenes. *J. Org. Chem.* **2016**, *81*, 2635-2638. (d) Vásquez-Céspedes, S.; Wang, X.; Glorius, F. Plausible Rh(V) Intermediates in Catalytic C–H Activation Reactions. *ACS Catal.* **2018**, *8*, 242-257.

(22) (a) Gorelsky, S. I.; Lapointe, D.; Fagnou, K. Analysis of the Concerted Metalation-Deprotonation Mechanism in Palladium-Catalyzed Direct Arylation Across a Broad Range of Aromatic Substrates. *J. Am. Chem. Soc.* **2008**, *130*, 10848-10849. (b) Lapointe, D.; Fagnou, K. Overview of the Mechanistic Work on the Concerted Metallation–Deprotonation Pathway. *Chem. Lett.* **2010**, *39*, 1118-1126. (c) Wu, J.-Q.; Zhang, S.-S.; Gao, H.; Qi, Z.; Zhou, C.-J.; Ji, W.-W.; Liu, Y.; Chen, Y.; Li, Q.; Li, X.; Wang, H. Experimental and Theoretical Studies on Rhodium-Catalyzed Coupling of Benzamides with 2,2-Difluorovinyl Tosylate: Diverse Synthesis of Fluorinated Heterocycles. *J. Am. Chem. Soc.* **2017**, *139*, 3537-3545.

(23) Yu, J.-L.; Zhang, S.-Q.; Hong, X. Mechanisms and Origins of Chemo- and Regioselectivities of Ru(II)-Catalyzed Decarboxylative C–H Alkenylation of Aryl Carboxylic Acids with Alkynes: A Computational Study. *J. Am. Chem. Soc.* **2017**, *139*, 7224-7243.

(24) For the detailed DFT results of paths **I**, $\mathbf{I_a}$ and $\mathbf{I_b}$ in DCM and paths **II**, $\mathbf{II_a}$, and $\mathbf{II_b}$ in methanol, please see figures 2-3; for the detailed free energy profiles of both disfavored path **II** (in DCM) and the disfavored path **I** (in methanol) that select as the rate-determining steps, please see the

Supporting Information. For the summary results, please see figure 4.

(25) (a) Huo, C.; Xu, X.; An, J.; Jia, X.; Wang, X.; Wang, C. Approach to Construct Polysubstituted 1,2-Dihydronaphtho[2,1-b]furans and Their Aerobic Oxidative Aromatization. *J. Org. Chem.* **2012**, *77*, 8310-8316. (b) Shen, H.; Fu, J.; Yuan, H.; Gong, J.; Yang, Z. Synthesis of 2,3-Disubstituted Indoles and Benzofurans by the Tandem Reaction of Rhodium(II)-Catalyzed Intramolecular C-H Insertion and Oxygen-Mediated Oxidation. *J. Org. Chem.* **2016**, *81*, 10180-10192.

TOC Graphic